New achievements in underwater noise modelling for offshore pile driving

Benjamin TRIMOREAU[1]; René Smidt LÜTZEN[2]; Jon VINDAHL KRINGELUM[3]; Amir SHAJARATI[4]; Peter SKJELLERUP[5]

[1,2] Lloyd's Register Consulting, Denmark

[3,4] DONG Energy Wind Power, Denmark

[5] Geocos, Denmark

ABSTRACT

Underwater noise emission from pile driving within the offshore wind industry is becoming an increasingly important issue. To advance the understanding and ability to predict underwater noise emissions and associated control measures, Lloyd's Register Consulting and DONG Energy Wind Power have initiated model development activities. Two procedures have been applied. First a technique based on empirical data and long range sound transmission models was successfully evaluated. The prediction is based on a semi-empirical source strength which may be re-used for another site, provided the piling setup is similar. Second, a modelling method was then initiated to account for any hammer and pile configurations and gain knowledge on the near-field sound generation. The method combines two techniques: stress-Wave Equation Analysis for Piles (WEAP) and vibro-acoustic Finite Element (FE). WEAP is a well-established geotechnical tool that calculates the stress wave in the hammer-pile system. A customized WEAP is implemented in order to output soil damping and loading function information. The time-domain FE model is then set up accordingly and predicts acoustic pressure data in the vicinity of the pile. Comparisons to measured hydrophone data are very promising and that bodes well for the next modelling steps.

Keywords: Underwater, Piling, Modelling I-INCE Classification of Subjects Number(s): 54.3

1. INTRODUCTION

The current focus on offshore wind energy in Europe - in connection with EU's energy policy objectives and the aim to reduce Cost of Energy – brings up a number of new technical focus areas and associated challenges. One of them is the installation of foundations for wind turbines involving a variety of foundation technologies and thorough logistics. In the German Exclusive Economic Zone (EEZ), monopile foundations are commonly employed as a well proven and robust solution. These and other types (e.g. jackets and tri-piles) are mainly installed via hydraulic pile driving. Recent publications (1,2) show that the transient load creates a stress wave in the steel pile - reflecting back and forth between the pile ends – which generates high-pressure acoustic waves in the water and seabed via radial expansion.

The Federal Ministry for the Environment, Nature Conservation and Nuclear safety (BMU) has set noise requirements in the German EEZ at a distance of 750 m to the pile. The limits are 160 dB re1µPa^2.s in terms of sound exposure level (*SEL*) and 190 dB re1µPa in terms of peak-to-peak levels

Reported measurement results show that for unmitigated driving of large diameter piles, these limits are often exceeded (e.g. 3-5), thus introducing challenges and uncertainties into the installation process. This calls for an accurate, validated prediction tool to more precisely quantify this. Such a

[1] benjamin.trimoreau@lr.org
[2] rene.smidtluetzen@lr.org
[3] jonvk@dongenergy.dk
[4] amish@dongenergy.dk
[5] ps@geocos.dk

tool is also needed as background for assessing the effect of noise mitigation methods, prior to the actual construction. The task of establishing a reliable prediction tool is presently pursued by Lloyd's Register Consulting and DONG Energy Wind Power.

Two different numerical techniques are presented in this paper and validation is carried out based on measured hydrophone data from full-scale pile-driving test cases. The first method predicts long-range noise levels based on sound transmission models and empirical sound transmission data. The applicability of a monopole source assumption combined with a numerical propagation model is examined in (6), and the present study relies on airgun based measurements of transmission loss, combined with a Wavenumber Integration type propagation model.

The second technique is more detailed and accounts for the dynamics within the hammer-pile system and the energy dissipation mechanism at the pile-soil interface. The aim is for a prediction in absolute terms, based on technical site-specific inputs rather than empirical. The complexity of an embedded offshore pile seen as an acoustic source is met by detailed FE modelling. The pioneering work by Reinhall and Dahl (1) describes the detailed physics of the noise source. In (7) modelled and measured transfer functions are compared and the model is empirically adjusted in terms of friction loss. In (2, 8) the pile-soil energy losses are represented by means of distributed spring-damper elements, and furthermore the Finite Element near-field model is coupled with a long-range Wavenumber Integration model. The hammer force onto the pile in these contributions is approximated by a semi-analytical approach.

This second approach combines classic WEAP (Wave Equation Analysis for Piles) (9) and vibro-acoustic Finite Element (FE) methods. A WEAP type script is run prior to the FE model in order to provide the pile head loading function and seabed damping properties based on site-specific information.

2. TEST CASES

Two offshore pile driving experimental cases are considered in this study for validation purposes.

2.1 Case1: Anholt Offshore Wind Farm

Underwater noise of unmitigated pile driving was recorded in July 2012 at Anholt Offshore Wind Farm (OWF). The piling of two steel monopiles is treated in this paper, named P02 and P23. The monopile design is conical with varying wall thickness leading to a mean outer diameter of 5.3 m and mean wall thickness of 56 mm. Pile geometry and site conditions at each position is stated in *Table 1*. Bathymetry data show water depths varying maximum 0.5 m/km around the pile sites. An empirical, site-specific summer sound speed profile was extracted from the World Ocean Database (10) varying from 1500 m/s at the sea surface down to 1483 m/s towards seafloor. More site-specific geological inputs are presented in Sections 3.3 and 4.4.2.

Table 1 – Monopile dimensions and site data at Anholt OWF

Pile site	Length (m)	Final penetration depth (m)	Water depth (m)	Sediment type
P02	39.6	19.1	18	Silty sand / sand
P23	47.5	28.1	16.9	Sitly sand / clay / sand

The installation was operated from the barge crane Svanen, with the pile located inside the barge horseshoe shape. The employed hammer system was an IHC S-2000 Hydrohammer comprising a 100,000 kg ram, an anvil and an anvil ring. No cushion element was applied.

Four receiver stations were deployed on site as shown in Figure 1: one close to the installation vessel (circa 60 m distance), two at 750 m distance (90 degrees apart) and one at 1500 m distance. Each station consists of two hydrophones, respectively 3 and 10 m off the seafloor.

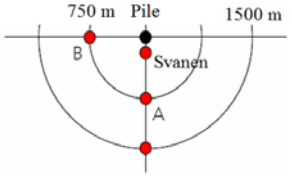

Figure 1 – Experimental hydrophone stations during the July 2012 measurement campaign.
The black dot indicates the pile location. Hydrophones were BK8101, BK8505, Reson 4013 and TC4032. In addition, air-gun noise was recorded at P02 with emphasis on calibration of the acoustic model

2.2 Case 2: Vashon Island ferry terminal

A comprehensive experimental setup of harbour piling from the Vashon Island ferry terminal is described in (1). In short, the cylindrical steel piles had length 31.9 m, outer diameter 0.76 m. They were driven to penetration depth of 14 m at water depth 12.5 m in a sandy soil. The pile was driven by a diesel hammer, Delmag D62-22 with a 6,200 kg ram. No cushion element was used. The reported hammer energy is 180 kNm.

Underwater noise was recorded close to the pile using a vertical line array (VLA) of hydrophones at ranges 8, 12 and 15 m from the pile.

3. SEMI-EMPIRICAL LONG-RANGE MODELLING

3.1 Method

The modelling technique presented here builds on (6). Measured acoustic pressure data at long range (> 500 m) is combined with a sound transmission model to reconstruct a source level at 1 m. The outcome is a semi-empirical equivalent monopole source level. For piling noise, a standardised source level definition is not yet agreed, partially due to complications of the source being integrated with the medium, see e.g. (11). In the present study, however, a simple approach is discussed with focus on unmitigated piles.

First the acoustic properties of the site-specific layered seabed (so-called geoacoustic model) are adjusted based on empirical acoustic pressure signals of air-gun shots fired close to the considered pile location. Adjustment are based on physical reasoning from inspection of Transmission Loss (TL) data, defined per 1/3 octave band as

$$TL(r,d) = ES_r(r,d) - ES_s(r,d) \quad (1)$$

Here $ES_{r,s}$ is the energy spectrum level per 1/3 octave (in dB re 1μPa^2.s) at range r [m] and depth d [m] at the source and receiver, respectively. The energy spectrum is also called *SEL* spectrum and its overall value corresponds to the *SEL* metric used in the German EEZ noise regulations. Peak-to-peak levels (L_{pp}) are also predicted in this study based on an empirical relation between *SEL* and L_{pp} data.

The updated geoacoustic model is supplied to a new transmission model and the TL data are combined with long-range piling noise signals to reconstruct a source spectrum ES_{1m}

$$ES_{1m}(r,d) = ES_r(r,d) - TL_{ref\,1m}(r,d) \quad (2)$$

Here ES_r is taken from a received pile signal at a station at long range. TL_{ref1m} is the computed TL data for the studied pile site, assuming a certain monopole depth. For ES_r, penetration depth and hammer energy are associated from the hammer log data. These parameters along with hammer configuration and pile-soil interaction directly affect the extracted source level. Hence, the prediction site must have similar properties in terms of geology and hammer system as the site for which the source level was originally derived.

For better accuracy, the calculations of equations (1) and (2) are done in a finer resolution (e.g. 1/12 octave) and subsequently integrated into 1/3 octave. Validation of the method is carried out by reusing the source level at another pile site and compare predicted vs. measured long-range *SEL* and L_{pp} data.

3.2 Model Components

Various low-frequency propagation models for TL are available that solve the fundamental Wave Equation at long ranges e.g. (13, 14). These well-established models use the monopole noise source representation.

The sites P02 and P23 at Anholt OWF can be considered as practically range-independent in terms of seafloor slope. The wavenumber integration program Scooter and Fields (14), which is inherently range independent, was applied. The model generates a 2D slice (range vs. depth) of TL data from the noise source, assuming azimuth-independency.

3.3 Results

3.3.1 Geoacoustic model refinement

Geoacoustic models were established for the two positions considered at Anholt OWF from Cone Penetration Testing data and area geology, involving some uncertainty, particularly for attenuation. Three typical seabed layer types were defined with both compressional and shear wave properties. The

P02 and P23 environments consist of respectively 18 m and 16.9 m water columns on top of two and three soil layers, the lowermost being an infinite half-space.

Examples of air-gun shots from P02, off the side of the barge vessel are shown in Figure 2. An alternative TL definition was used with energy spectrum at 1500 m, referenced to 750 m (same receiver depth at both stations).

$$TL_{ref\,750}(1500,d) = ES_r(1500,d) - ES_s(750,d) \tag{3}$$

An analogue TL quantity is defined for Scooter and Fields data as

$$TL_{ref\,750}(1500,d) = TL_{ref\,1m}(1500,d) - TL_{ref\,1m}(750,d) \tag{4}$$

Modelled and measured TL data are compared for several pairs of air-gun depth / receiver depths. Measured data are spatially averaged on an energy basis around each receiver position.

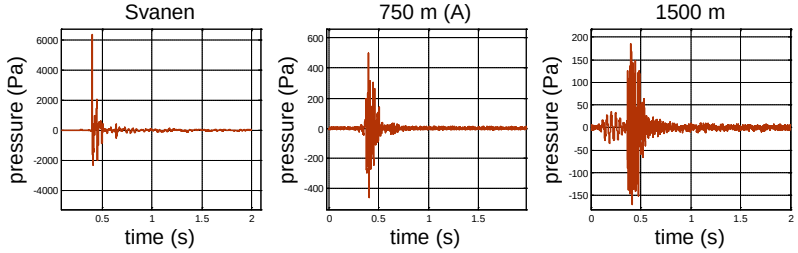

Figure 2 – Example of received acoustic pressure from air-gun shots (Pa vs. s) at P02 site: at the Svanen, 750 m (A) and 1500 m stations. Hydrophone depths are 2.5-3 m off bottom. Air-gun depth is at depth 7.5 m.

The empirical TL data, either using station A or B show differences up to 5 dB per third octave, probably due to reflections from the vessel. The mean of A and B data is used for comparison with the model. Inspection reveals lack of low frequency attenuation in the model and a head wave from a deep, high shear speed layer, hence deviating from a typical Perekis waveguide behaviour (12).

Iterations led to alternative lower compressional wave attenuations for the layers at P02. Compressional attenuation of the upmost 3 m layer at this site was found to have the greatest impact for the considered ranges. No rigid seabed was included, and hence the low frequency head wave phenomenon remained uncaptured.

3.3.2 Piling noise source level evaluation

The adjusted sound transmission model is run to provide TL referenced to 1 m. Equation (2) is then employed to evaluate a source spectrum referenced to 1 m. Following (6), a point source depth of 0.5 m above seafloor is applied in order to minimize Lloyd's mirror effect.

For P02, a set of measured pile strikes is selected having a pile penetration depth ca. 19 m and with associated hammer energy of 400 kNm. The spectral shape at 1 m using the different long-range data is consistent, and overall SEL varies within 2 dB, indicating a reasonable TL model.

A new TL model is set up for position P23 with geoacoustic properties adjusted according to the previous findings. A set of piling strikes at P23 is selected with similar hammer energy and penetration depth as for P02. The seabed composition here deviates slightly as the P23 seabed profile has more soft clayey layers. However, (15) shows that the noise radiated from the portion of an unmitigated pile in direct contact with the water dominates the propagating noise. Hence, the penetration depth and soil layering can differ to some extent in this approach. Measured vs. calculated long range spectra at P23 are given in Figure 3.

Comparison of the modelled data against measurements in Figure 3 shows that the approach is reasonable, with deviations within 2 dB in terms of overall *SEL*. The other sets of range and depth available give rise to similar level of consistency vs. the calculations. As for P02, a directivity feature between stations A and B is seen - indicating a degree of uncertainty around +/-3 dB.

Finally Peak-to-peak levels are calculated at P23 based on an empirical relation between overall *SEL* and Peak-to-peak levels L_{pp}. A regression expression is evaluated based on P02 hydrophone data and determined as $L_{pp}=1.25 \cdot SEL-15.2$. Similarly to the *SEL* data, modelled L_{pp} at P23 agree within 2 dB when compared to measured data.

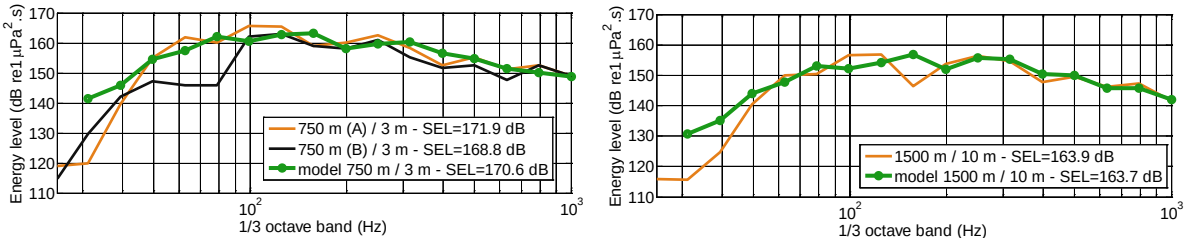

Figure 3 – Measured vs. modelled energy spectrum per 1/3-octave at P23. Pairs of receiver range/depth are: 750 m and 3 m off seafloor (left) and 1500 m and 10 m off seafloor (right). The model is based on the source spectrum extracted at P02. Hammer energy is 396 kNm and penetration depth is 13 m at P23.

This long range technique for evaluating *SEL* and L_{pp} of unmitigated piling noise seems to perform well. The method is however, limited since source spectra represent a specific piling configuration.

4. WEAP-FE Modelling Technique

An alternative modelling procedure is proposed which relies on combining two techniques that are separately well-established: Wave Equation Analysis for Piling (WEAP) and Finite Element (FE). Both have strengths and shortcomings, and the combined method aims at exploiting the former. WEAP is used to produce two parameters: The loading time function from the hammer system onto the pile head, and the damping ratio corresponding to the dissipated energy at the pile-soil interface. These are used as input to the vibro-acoustic FE model.

4.1 Introduction to WEAP

WEAP type models have been used by the geotechnical community for decades to estimate the necessary hammer size in order to obtain a given penetration depth for a given soil and pile size – and the driving induced pile stresses. A classic WEAP model represents the interaction between an impact hammer, pile, and soil.

The stress-Wave Equation Analysis for Piling first introduced by Smith (9) is a time-domain, finite-difference approach to the wave equation based on longitudinal wave propagation in the pile. The full derivation is given in (16). The one-dimensional wave equation is given as (17):

$$\frac{\partial^2 D}{\partial t^2} = \left(\frac{E}{\rho}\right)\left(\frac{\partial^2 D}{\partial x^2}\right) \pm R \tag{3}$$

Here, E is the modulus of elasticity of the pile, ρ is the density of the pile material, D is the longitudinal displacement of a point on the pile from its original position at location x and time t, and R is a soil resistance term. The principle of discretisation of the entire dynamic system is shown in *Figure 4*, where the "capblock" represents any component between ram and pile head.

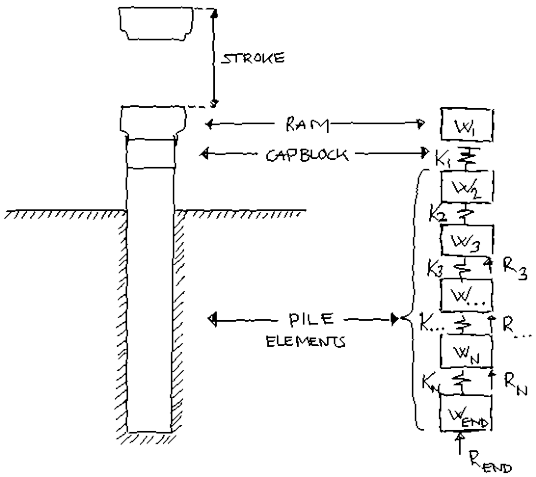

Figure 4 – Classical discretisation of hammer, pile and soil by means of lumped elements (18).

At each pile element n embedded in the soil, the soil resistance R_n [N] is comprised by:

$$R_n = R_{s,n}(1 + J_n \cdot v_n) \tag{4}$$

Here $R_{s,n}$ is the soil spring force at element n, which is represented by an elasto-plastic load-deformation relation. J_n [s/m] is the "Smith damping coefficient", and v_n [m/s] is the pile velocity. The soil spring force is derived from the maximum static resistance of the soil and the maximum elastic deformation (quake) Q_n [m]. Note from equation (4) that J is multiplied both by the spring force and the velocity.

The parameters Q and J are nonstandard soil mechanics parameters and various alternative representations particularly of the damping have been investigated (see e.g. (17, 19)). However, Smith's formulation has proven relatively robust and experience from decades of use within the geotechnical community has provided narrow bands on the parameter values (19). Hence, Smith's formulation is kept for the present study.

4.2 Combined Method of WEAP and FE

In (20) the radial expansion from a WEAP model is treated as the amplitude of an array of idealised dipole-sources and coupled with an acoustic propagation model. The present approach exploits the vibro-acoustic coupling of an FE model, while relying on WEAP for detailed estimation of hammer force and energy dissipation. Hence, a relatively simple, axisymmetric time-domain FE model is established which is linear and includes only the pile structure, the water, and the seabed. The pile-soil interaction is not modelled directly. Instead, the soil is modelled as a fluid and the energy dissipation is represented using Rayleigh damping assigned to the embedded part of the pile (7, 21). Then, the resulting acoustic field in the water and seabed is computed by the FE model.

4.3 Model Components

4.3.1 Customised WEAP

In addition to the classic WEAP discretisation of *Figure 4* it was decided to add material damping within the pile and hammer system. Hence, a viscous damping force is introduced between each element, acting in parallel with the spring force.

For a geotechnical context, relatively coarse resolution of time and space (e.g. 0.1 ms and 1 m) usually suffice. However, for the present acoustic purposes a significantly finer resolution has proven necessary to sample the wave propagation within the hammer components, particularly for uncushioned systems. Attention needs to be drawn to numerical stability.

WEAP models axial wave propagation, while for acoustics the radial pile expansion (or displacement) y [m] is required. Inspired by (20), y is approximated as $2 \cdot \nu DC/L$ for a cylindrical pile element, where ν is Poisson's ratio, D [m] the element diameter, C [m] the axial compression, and L [m] the undisturbed length.

To obtain the pile head loading as a function of time a WEAP model run is performed with a pile length sufficiently long that reflections from the pile toe are not observed. The pile head loading is then extracted as the contact force between pile head and hammer system.

To express the energy dissipation in a suitable manner for the FE model, the WEAP model is run using the actual pile length. For each element this produces time series of radial displacement y that are inspected using Fourier spectrograms. From these the various dominant frequencies f_i [Hz] corresponding to reflected-reflected wave patterns are easily identified. A zero-phase band-pass filter is applied to each, and equivalent viscous damping ratios ξ_i are evaluated using a decay technique. This results in pairs of dominant frequencies and damping ratios. The method seems fairly robust even for the slightly non-linear WEAP data. Next, the energy loss data are converted to Rayleigh damping format described by two parameters α [s] and β [s^{-1}], which are the mass and stiffness proportionality coefficients, respectively. Selecting two frequency/damping pairs f_i, ξ_i allows simple algebraic solution for α and β, and hence the Rayleigh damping (18).

4.3.2 Vibro-Acoustic FE Model

The time-domain FE model using the ABAQUS/Explicit package is 2D axi-symmetric as employed in (1), (2) or (7). A structural mesh is set based on 4-node elements with a seed size evaluated to compute acoustic energy up to roughly 1.5 kHz. The seabed layers are composed by fluid elements. Hence, shear propagation and soil internal friction are not implemented.

The sea surface is modelled as a perfect reflector using a pressure release boundary condition, and

the air domain is not modelled. Non-reflecting boundary conditions are applied to mimic the far-field propagation.

The hammer system is not modelled directly, but represented by the pile head loading time series from WEAP. The energy dissipation at the soil-pile interface is modelled via Rayleigh damping parameters from WEAP, assigned to the embedded pile part. The resulting sound field in the pile surroundings can now be sampled at any grid position.

4.4 Results

4.4.1 Case 2: Vashon Island case

Two distinct WEAP runs supplied respectively the force time series onto the pile head and the radial displacement time series at discrete positions of the pile. The latter for derivation of soil damping as explained in Section 4.3.1. The inputs to WEAP are based on the available site information (see 2.2) of the hammer details and pile geometry. The initial ram velocity is 7.6 m/s (1) and the hammer components are represented by 5 elements. No detailed information on seabed type and damping is available for this site and two coarse cases of Smith's damping constant are examined. The first case assumes a more cohesive soil ($J=J_{toe}$=0.5 s/m), whereas the other a dense sandy soil ($J=J_{toe}$=0.2 s/m). Generic input data are then used along pile shaft and toe such as the ultimate static soil resistance (R_u=60 kN and R_{utoe}=1 MN) and "quake" values ($Q=Q_{toe}$=2.5 mm).

The customised WEAP assumes a gravity hammer whereas the actual diesel hammer provides rapid retraction of the ram. Hence, ram rebounds present in the computed force series are carefully removed prior to using it in the FE model.

Figure 5 presents a timeframe of the noise field from FE as well as computed time series and 1/3-octave energy spectra vs. measurements. The comparison in 1/3-octaves is only indicative since the measured spectra result from digitized, interpolated time series data. The terminology of (1) for the wave front arrivals is used here, i.e. phase I being the primary wave front, phase II the pile toe reflected wave front, phase III the pile head reflected wave front, etc. The FE domain size is set to 26 m from the pile outer wall and 8 m from the pile toe.

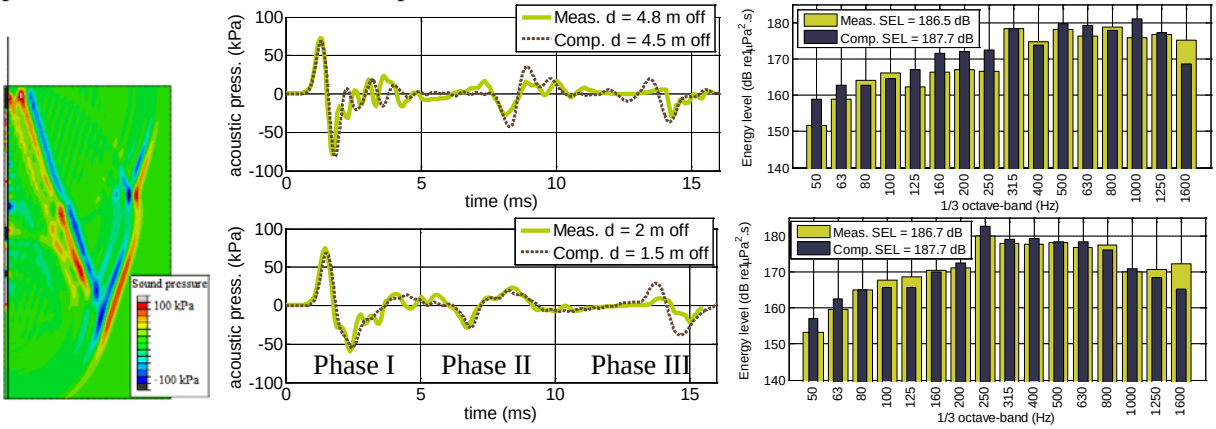

Figure 5 – Results of the WEAP-FE technique at Vashon Island site: FE sound field at t=13 ms (left), measured (digitized from (1)) vs. computed hydrophone time series for two depths off seafloor (middle) and corresponding 1/3-octave energy spectra (right). The FE receiver depths are within +/-0.5 m from the experimental ones, and all at range 12 m from the pile outer wall.

The computed time series in *Figure 5* show good agreement with measurements for phase I, which is governed by the force function input as the downward propagating wave front at this range has only interacted with the water. This in itself indicates validity of the applied driving system representation.

Phases II and III show slight deviations in amplitude between computed and measured data and a good match in arrival times. The results in frequency domain are satisfactory, leading to good agreement in overall *SEL* around +/-1 dB. Here, the *SEL* values were not computed from the pulse duration but over the entire signal length and at a very close range of 12 m.

The dense sandy soil case of Smith's damping constant was applied in the WEAP run and led to a poorer match for the FE time series vs. measurements for phase II and III. The comparison vs. empirical data was still reasonable in terms of *SEL* with deviations within +/-3 dB.

In the light of the lacking geotechnical data, the investigated damping values show that using these common values provide good results. While this is not a perfect validation case, the WEAP-FE approach seems promising.

4.4.2 Case 1: Anholt OWF case

The WEAP-FE procedure is carried out for pile P23 at Anholt OWF and different penetration depth cases using site-specific geotechnical data. As mentioned in Section 3.3, the sound field at this site is affected by features such as hard wall reflections, which are not modelled in the 2D FE simulations. This complicates comparison to measured data. Properties of certain hammer components were carefully assessed using FE. The conical pile profile is modelled in WEAP whereas a mean diameter and wall thickness are employed in the acoustic FE model.

Several penetration depths are simulated. An example of computed pile head force using WEAP is given in *Figure 6* left – corresponding to the spring force located above the pile head.

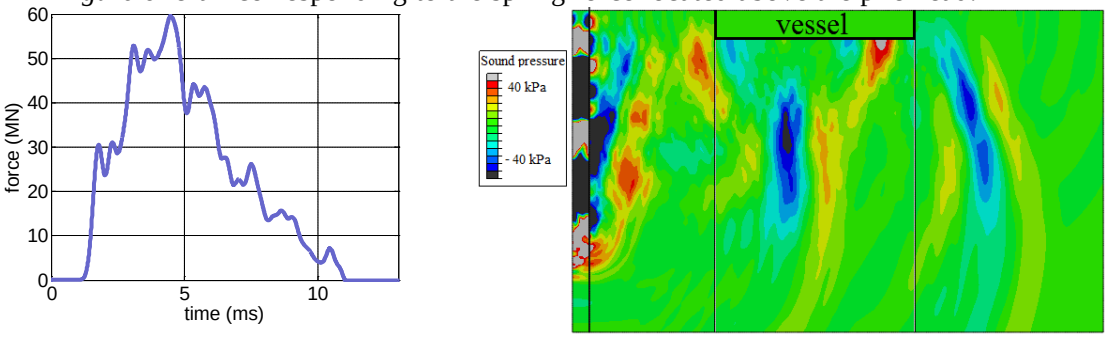

Figure 6 – Pile head force vs. time from at P23 for a penetration depth of 10.1 m, hammer energy 295 kNm (left)and sound field from FE at P23, at 49 ms time step and penetration depth of 18.1 m (right). The added steel region is visible and was placed roughly 20 m from the pile with height 4.5 m high and width 31m (labelled "Vessel"). Receivers were placed a few meters right of the hull outer edge.

The curve character in *Figure 6* (left) differs from semi-analytical curves based on e.g. exponential regressions. The details illustrate the actual hammering dynamics.

Part of the Svanen barge hull is included in the FE geometry to account for the forward surface reflections (the even wave front phase numbers in (1)). Other non-symmetric reflectors are not included at this stage of the study.

Figure 6 right shows an example of the FE sound field. The FE domain extends 80 m from the pile outer wall and 15 m below pile tip. The fluid seabed follows the P23 3-layer layout of Section 3.3.1.

The deployment range of the hydrophone contains some uncertainty and is 60 m +/-10 m whereas the depth is 14 m +/-1m. *Figure 7* shows the computed acoustic time series and 1/3-octave energy spectra vs. empirical data, for two penetration depth cases. For the considered distance, the wave fronts have already interacted either with the seafloor interface (initial downward going waves, i.e. odd phase numbers) or the sea surface / barge hull (initial upward going waves, i.e. even phase numbers). The resulting waveform at 60 m is hence affected by the impedance mismatch between water and seafloor. Changing slightly the p-wave speed of the top seabed layer leads to a different reflected wave angle and therefore a modified sound field at the receiver position. Also, complex interference patterns arise from the different wave fronts made of positive-negative pairs.

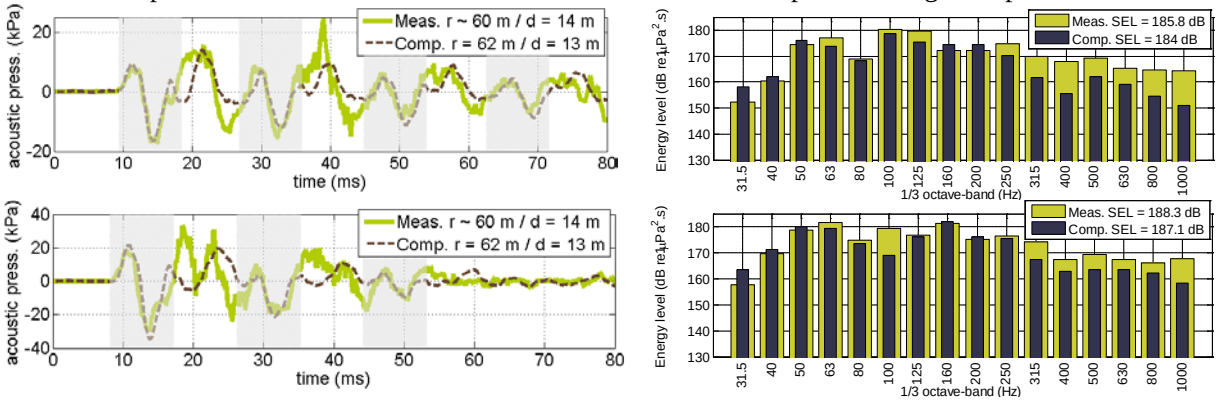

Figure 7 - Results of the WEAP-FE method at P23 site, Anholt OWF: measured vs. computed hydrophone time series and 1/3-octave energy spectra for a penetration depth of 10.1 m (top) and 18.1 m (bottom). Numerical receiver range and depth are identical for both FE runs and are within +/-2 m from the measured ones. Grey regions correspond to the odd phase numbers in (1).

As in the Vashon case study, the loading function supplied by WEAP seems to work well since

phase I is well captured for both modelled time series. The subsequent odd phases (greyed zones in the time plots) follow the same pattern for both penetration depths, and agree well with the empirical curves. These phases include energy dissipation within the embedded pile part. The result shows that the damping model is reasonable. Indeed, consistent decaying behavior between modelled and measured data is observed for both penetration depths.

On the other hand, all upward moving wave fronts match poorly, most likely due the onsite interference of the asymmetric Svanen hull. Particularly for the 10.1 m case a spike is observed in the measured signal at 39 ms. The data for the final penetration depth (28.1 m) are not shown here but pointed out even poorer match for the even phases supporting that the current seabed representation in the FE model is too poor and tend to collapse towards greater penetration depths.

Investigations are ongoing regarding the origin of the extra interactions with the barge hull as well as the impact of refining the seabed representation. Of note is that the air-gun based transmission loss data support the hypothesis of hull reflections, rather than e.g. hammer re-strikes.

The computed 1/3-octave spectra point out deviations in amplitude – due to the non-modelled 3D features – but show similar frequency contents. The overall SEL agree then within +/- 2 dB.

5. Conclusions

The steadily increasing activity within offshore wind is creating awareness of underwater noise, particularly related to the installation of piles. Many aspects of the noise generation physics are still not fully understood which introduces uncertainty into the industry. The present paper assists in meeting this shortcoming by presenting two modelling approaches, one semi-empirical for long range propagation, and a quantitative model for near-field ranges.

Long range propagation models often assume monopole source, which in general has limited validity for an embedded pile. However, for unmitigated piles at similar geotechnical conditions e.g. within the same offshore wind farm (OWF) and similar pile driving conditions, a practical site specific method is described in this contribution. The on-site transmission loss data based on an air-gun signal proved useful for calibrating a detailed propagation model. Also, an equivalent source description to be used with the propagation model was determined. This approach was applied to full-scale test data from the Anholt OWF and prediction at 750 m distance for a nearby pile location was compared to actual measurement data. Good agreement was shown for both Sound Exposure Level (*SEL*) and Peak-to-peak Level (L_{pp}), within +/-2 dB. During the adjustment of the propagation model, it was found that the largest sensitivity was in the geoacoustic parameters of the upper sediment layer, especially its compressional wave attenuation.

While the proposed long-range propagation model relies on site-specific empirical data, a qualitative approach was pursued that does not involve tuning against experimental data. The well-established geotechnical tool WEAP (stress-Wave Equation Analysis of Piling) was combined with the Finite Element (FE) method. Here, the strength of WEAP is twofold: The representation of the complex pile-soil interaction, and of the multi-component hammer systems common to offshore piling. The proposed method makes use of WEAP for estimating the related energy dissipation, and the loading to the pile head. By introducing these as input to a relatively simple FE model, an operational prediction method is achieved. Comparison was done to literature empirical data at 10 m distance from a small, driven harbour-pile. Geotechnical details were not given, but using common soil damping values returned overall levels that agreed with measurements within +/-1 to +/-3 dB. In the best case, good agreement of sound pressure time series as well as 1/3-octave band spectra was achieved.

The WEAP-FE approach was likewise tested against previously taken measurement data from the Anholt OWF. Here, the measurement distance was approximately 60 m, causing uncertainties from the test set-up to provide challenges. However, the parts of the received acoustic pressure time series relating to downward propagating stress waves in the pile showed good agreement with the measurements, in the order of +/-4-5 kPa. This indicates adequate representation of the hammer system and of the pile-seabed interaction. The parts of pressure time series relating to upward propagating stress waves involved interaction with the installation vessel, the position of which was not fully clear. Also, shortcomings of the fluid seabed assumptions were noted. Hence, some deviation compared to measurements was observed. Nevertheless, overall SEL agreed within 2 dB.

Seen as a new approach to quantitative prediction of piling noise, the WEAP-FE method appears promising. More validation cases against real-world data should be examined. Furthermore, future work is relevant for integrating near field and long range modelling, such as initiated in (8). Also, alternative seabed representation in FE using continuum type elements is currently being investigated.

ACKNOWLEDGEMENTS

The authors gratefully acknowledge the collaboration with Maiken Bruun-Ringgaard during her MSc Thesis work on a WEAP-FE approach.

REFERENCES

1. Reinhall PG, Dahl PH. Underwater Mach wave radiation from impact pile driving: Theory and observation. J Acoust Soc Am. 2011;130(3):1209-1216.
2. Lippert S, Lippert T, von Estorff O. Prediction of underwater sound due to pile driving for offshore wind farms - A challenge for numerical simulation. Proc INTER-NOISE 2012; 19-22 August 2012; New-York, USA 2012.
3. Matuschek R, Betke K. Measurements of Construction Noise During Pile Driving of Offshore Research Platforms and Wind Farms. Proc NAG/DAGA International Conference on Acoustics; 23 - 26 March 2009; Rotterdam, the Netherlands. pp. 4
4. Robinson SP, Theobald PD, Lepper PA. Underwater noise generated from marine piling. Proc Meetings on Acoustics, 2013; 17.
5. Bellmann MA, Gündert S, Remmers P. Offshore Messkampagne 1 (OMK 1) für das Projekt BORA im Windpark BARD Offshore 1. Report for the BMU funded research project “Predicting Underwater Noise due to Offshore Pile Driving (BORA)”, 2014 February. Project ref. no. 0325421 A. Oldenburg, Germany.
6. Duncan AJ, McCauley RD, Parnum I, Salgado-Kent C. Measurement and Modelling of Underwater Noise from Pile Driving. Proc 20th International Congress on Acoustics, ICA 2010; 23 – 27 August 2010; Sydney, Australia 2010.
7. Zampolli M, Nijhof MJJ, de Jong CAF, Ainslie MA, Jansen EHW, Quesson BAJ. Validation of finite element computations for the quantitative prediction of underwater noise from impact pile driving. J. Acoust Soc Am. 2013; 133(1):72-81.
8. Lippert T, von Estorff O. On a Hybrid model for the Prediction of Pile Driving Noise from Offshore Wind Farms. In: Acta Acust united Ac. 2014; 100: 244 – 253.
9. Smith EA. Pile-Driving Analysis by the Wave Equation. Journal of the Soil Mechanics and Foundations Division, August 1960, pp. 35-61. New York: ASCE.
10. National Oceanographic Data Center (NODC). National Oceanic and Atmospheric Administration (NOAA) World Ocean Database [Internet]. 2006 [Cited 5 June 2013]. Available from: http://www.nodc.noaa.gov/OC5/SELECT/dbsearch/dbsearch.html
11. Ainslie MA, de Jong CF, Robinson SP, Lepper PA. What is the Source Level of Pile Driving Noise in Water? In: Popper AN, Hopkins A, editors. The Effects of Noise on Aquatic Life: Advances in Experimental Medicine and Biology. 2012; 730(VII): 445-448.
12. Jensen FB, Kuperman WA, Porter MB, Schmidt H. Computational Ocean Acoustics. 2nd ed. New York, USA: Springer; 2011.
13. Collins MD. Users Guide for RAM versions 1.0 and 1.0p. Washington, USA: Naval Research Laboratory; 1999.
14. Porter M. Acoustic Toolbox [Internet]. 2005 [updated 1 Sept 2010; cited 9 July 2014]. Available from: http://oalib.hlsresearch.com/Modes/AcousticsToolbox/
15. Stokes A, Cockrell K, Wilson J, Davis D, Warwick D. Mitigation of Underwater Pile Driving Noise During Offshore Construction: Final Report. Groton, USA: Applied Physical Sciences; 2010. Report no. M09PC00019-8
16. Forehand PW, Reese JL. Pile Driving Analysis Using the Wave Equation [M.Sc. thesis]. Princeton, USA: Princeton University; 1963.
17. Poulos HG, Davis EH. Pile foundation Analysis and Design. New York, USA: Wiley; 1980. p.59-70.
18. Bruun-Ringgaard M. Modelling of underwater noise from pile driving [MSc thesis]. Lyngby, Denmark: Technical University of Denmark, Department of Electrical Engineering; 2014
19. Randolph MF. Analysis of the Dynamics of Pile Driving. In: Banerjee PK, Butterfield R, editors. Advanced Geotechnical Analyses. London, UK: Taylor Francis; 2011. p. 223-272.
20. Wood M, Humphrey V. Modelling of Offshore Impact Piling Acoustics by Use of Wave Equation Analysis. Proc 1st ICEUA; 23-28 June 2013; Corfu, Grece 2013. p. 171-178
21. Fritsch M. Zur Modellierung der Wellenausbreitung in dynamisch belasteten Pfaehlen [Ph.D. thesis]. Braunschweig, Germany: The Technical University; 2008. German.